Asian Journal of Chemistry; Vol. 25, No. 11 (2013), 6298-6302

ASIAN JOURNAL OF CHEMISTRY

http://dx.doi.org/10.14233/ajchem.2013.14427

Sintering Characteristics of Ceramsite Manufactured from Blast Furnace Slag and Sewage Sludge

Z.L. WANG[1,2]

[1]School of Civil Engineering, Nanjing Forestry University, Nanjing, Jiangsu Province, P.R. China
[2]College of Environment, Hohai University, Nanjing, Jiangsu Province, P.R. China

Corresponding author: Tel: +86 25 85427691, E-mail: wangzhulai@126.com, wangzhulai66@yahoo.com

(*Received*: 10 August 2012; *Accepted*: 8 May 2013) AJC-13459

To develop the recycling of solid wastes, blast furnace slag (BFS) and sewage sludge (SS) were added as components for making ceramsite. This study examined the sintering characteristics of ceramsite at different sintering temperatures and duration and different mass ratios (BFS: SS: clay). The results show that as the sintering temperature and duration increased, the pore size diameter gradually increased up to the maximum of 120 nm at 1100 ºC, 20 min. The turn point of the pore size diameter was at 1050 ºC, 20 min. Corresponding to the variation of the pore size diameter, the highest and lowest porosity of ceramsite reached 88 % and 62 %, respectively. The different mass ratios of three raw materials (BFS, SS and clay) had no obvious effect on the thermal behaviours of ceramsite and mostly the same trends of variation appeared in the curves of DT-TG. With the sintering temperature increasing, the complex crystalline phases appeared at 900 ºC and no variation happened on the main crystalline phases except the transformation from akermanite ($Ca_2MgSi_2O_7$) to gehlenite [$Ca_2Al(AlSiO_7)$] at 1050 ºC.

Key Words: Ceramsite, Blast furnace slag, Sewage sludge, Sintering characteristics.

INTRODUCTION

With the rapid economic growth of modern society, solid wastes as by-products of industry, household and agriculture are produced more and more every year across the world. In view of the development of regenerative resources, researches on management and recycling of solid wastes, especially industrial solid wastes were conducted in many countries and regions[1-4].

Blast furnace slag contains mainly inorganic constituents such as silica (30-35 %), calcium oxide (28-35 %), magnesium oxide (1-6 %) and Al_2O_3/Fe_2O_3 (18-258 %)[5]. Because of its simple components, studies on the recycling of blast furnace slag have been conducted in many fields including sorbents, packing or producing ceramsite with other solid wastes, *etc*. Blast furnace slag can be used as sorbents of phosphate for water solution. The kinetic measurements of adsorption confirmed that the sorption of phosphorus on crystalline as well as amorphous slags can be described by a model involving pseudo-second-order reactions. The phosphorus sorption followed the Langmuir adsorption isotherm[6]. Evaluation was done by comparing blast furnace slag samples with natural eelgrass sediment in terms of some physico-chemical characteristics and then, investigating growth of eelgrass both in blast furnace slag and natural eelgrass sediment[7]. Steel works slags can be blended with municipal sewage sludge for making ceramic specimens, which are sintered in air using a muffle furnace and characterized by density, strength, hardness, fracture toughness measurements, X-Ray diffraction and SEM investigations[8].

Sewage sludge is one of the final products of the treatment of sewage at wastewater treatment plants and usually contains high levels (10 % to >20 %) of organic matter and rich N and P that are essential for plant growth[9]. Owing to its characteristics, sewage sludge can be used to produce ceramsite alone or blend with other solid wastes. Sintering temperature had a significant effect on the characteristics of sludge ceramsite and that 1000 ºC was the optimal sintering temperature[10,11]. Wastewater sludge and drinking-water sludge could be mixed for making ceramsite. Fe_2O_3, CaO, MgO, SiO_2 and Al_2O_3 are the major basic oxides in them and the optimal contents of Fe_2O_3, CaO and MgO ranged 5-8 %, 2.75-7 % and 1.6-4 % and the optimal ratios of $(Fe_2O_3 + CaO + MgO)/(SiO_2 + Al_2O_3)$ ranged 0.175-0.45[12,13]. Dry sewage sludge can be also blended with coal ash to produce lightweight aggregate. Using dry sewage sludge enhanced the pyrolysis-volatilization reaction due to its high organic matter content and decreased the bulk density and sintering temperature. Adding coal ash improved the sintering temperature while effectively decreasing the pore size and increasing the compressive strength of the product[14].

The objective of this paper is to evaluate the feasibility that blast furnace slag was blended with sewage sludge for manufacturing ceramsite, which was sintered to observe the variation of its pores structure, thermal behaviours and crystalline phases at different temperatures and duration.

EXPERIMENTAL

Blast furnace slag in this study was obtained from the first energy factory of MA STEEL group, which is located at MaAnShan city in China. Blast furnace slag is produced by water quick cooling in the process of steelmaking in blast furnace. Sewage sludge was produced from dewatering workshop of Jiangxinzhou wastewater treatment plant located at Nanjing city in China. In this plant, primary sedimentation basin, A/O and secondary sedimentation basin are the major wastewater treatment technology and the sludge dewatered by pressure filter came from the excess sludge of secondary sedimentation basin. Clay was obtained from the work site in the 3rd Bridge of Yangtze river, Nanjing, China and the plasticity index of clay was over 17.

The chemical compositions of three raw materials mentioned above are shown in Table-1.

TABLE-1
ELEMENTAL ANALYSES

Elements	Si	Ca	Al	Mg	Fe	K	Na	P	Sb
BFS (w-%)	10.06	19.05	6.20	3.78	0.77	0.59	0.31	0.13	4.26
SS (w-%)	9.24	1.39	2.97	0.53	3.68	1.48	0.22	0.33	0.42
Clay (w-%)	16.68	0.69	6.28	0.78	3.19	0.99	0.63	0.05	-
	Mo	Sn	Ti	Mn	Cd	Se	Pd	O	C
BFS (w-%)	1.94	1.94	0.56	0.16	0.02	-	-	45.48	4.75
SS (w-%)	1.09	1.64	0.32	0.07	-	0.10	0.09	30.69	45.69
Clay (w-%)	0.07	1.10	0.33	-	-	-	-	52.08	17.13

The raw materials were ground by SF-130C pulverizer (Zhong Cheng Pharmaceutical Factory, JiShou City, China) at sizes below 100 mm to be well mixed. Three different dry weight ratios of slag: sludge: clay were evaluated in the following experiments as shown in Table-2. Every sort of ratio was defined as SSA, SSB, SSC, respectively.

TABLE-2
PERCENTAGE CONTENT OF THREE RAW MATERIALS OF CERAMITE

Sorts of ceramite	BFS (w-%)	SS (w-%)	Clay (w-%)
SSA	0	70	30
SSB	10	60	30
SSC	20	50	30

The raw materials were mixed and a DZ-60 pelletizing machine (Zhong Cheng Pharmaceutical Factory, JiShou City, China) was used to pelletize ceramsite with particle sizes of 4-6 mm and left in a room at a temperature of about 20 ºC for 4 days. Then the samples were dried at 105 ºC in a drying oven for 24 h. The examples of DT-TG analyses, namely SSA, SSB, SSC, were not preheated or sintered while the example of pore diameter structures and crystalline phase analyses, namely SSC, was first preheated at 400 ºC, 20 min and then sintered at different temperatures and duration. The chemical compositions of the raw materials were measured by electron energy disperse spectroscopy (INCA 250 EDS, UK). The pore diameter structures were conducted by mercury porosimeter (AutoPore 9510, US) at low pressure 30 psia and high pressure 60,000 psia. The thermal behaviour of products was examined by simultaneous DT-TG analyses instrument (diamond TG/DTA, US) when the examples were heated at a rate of 10 ºC/min from 30 to 1100 ºC in air. The crystalline phases of ceramsite were measured by X-ray diffractometer (D/max-2500/PC, Japan) with 50 mA and 40 kV.

RESULTS AND DISCUSSION

Effect of sintering temperature and duration on pore diameter structures of ceramsite: In order to examine the effect of sintering temperatures and duration on pore diameter structures of ceramsite, the example of SSC was sintered at different temperatures (900, 1000, 1050, 1100 ºC) and different duration (10, 20 min) after preheated at 400 ºC for 20 min. The results are shown in Fig. 1 and Table-3.

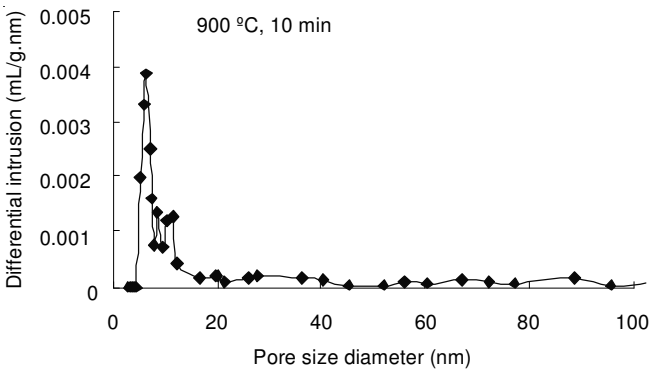

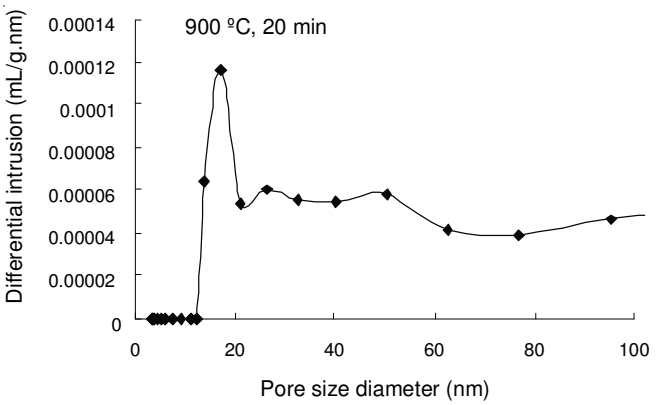

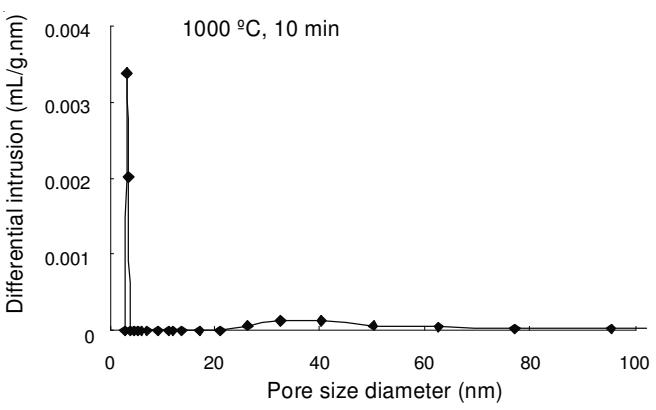

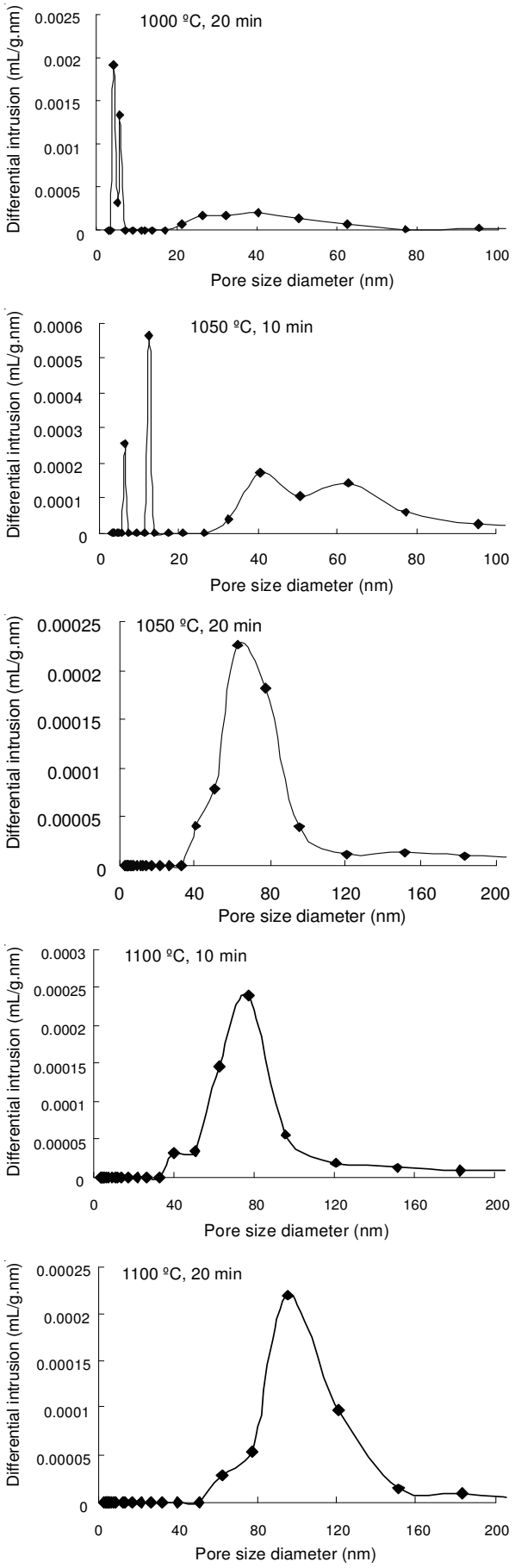

Fig. 1. Variation of pore diameter structure of ceramsite sintered at different temperatures and duration

TABLE-3
POROSITY VARIATION OF CERAMITE IN DIFFERENT SINTERING TECHNOLOGY

Sintering technology		Porosity (%)
900 ºC	10 min	88
	20 min	78
1000 ºC	10 min	64
	20 min	70
1050 ºC	10 min	77
	20 min	62
1100 ºC	10 min	63
	20 min	75

It can be seen from Fig. 1 that the small pores below 20 nm was the major pore structures before 1050 ºC, 10 min and the big pores over 20 nm always existed at 900 ºC, 10 min and 900 ºC, 20 min up to varying from 20 to 100 nm before 1050 ºC, 10 min; the major pore structures became larger than before and finally ranged steadily from 40 to 160 nm at 1100 ºC, 20 min; the pore diameters gradually increased when the sintering temperatures increased and the sintering duration varied from 10 to 20 min, respectively. The explanation of this phenomenon was that owing to the decomposition of organic matters producing CO_2, CO and C as the deoxidizer of Fe_2O_3 to form CO_2, a lot of small and big pores simultaneously appeared in the ceramsite before 900 ºC. From 1000 ºC, the small pores started melting to form big pores under the effect of fluxing agent, such as Fe_2O_3, CaO and MgO and the glass phases were finally produced resulting in the increasing compressive strength of ceramsite.

The porosity of ceramsite is a ratio of the volume of inner pores to total volume of the particle of ceramsite. Table-3 shows the variation of the ceramsite porosity at different sintering temperatures and duration. The highest porosity was 88 % that appeared at 900 ºC, 10 min and 62 % was the lowest porosity which appeared at 1050 ºC, 20 min. The low peak of porosity was shown twice at 1000 ºC, 20 min and 1050 ºC, 20 min, respectively. The first peak of 64 % was owing to the decreasing of small pores which were obtained from the release of CO_2 and CO. The melting of big pores and the forming of glass phases were the reasons of the appearance of the second peak of 62 %.

DT-TG analyses: To examine the effect of different mass ratios of three raw materials on the thermal behaviours of ceramsite, the examples of SSA, SSB, SSC heated from 30 to 1100 ºC in air were tested by DTA-TGA. The results are shown in Fig. (2a)-(2c).

It can be seen from Fig. (2a-2c) that the curves of DT-TG basically had the same variation except for a little difference from 800 to 1000 ºC in Fig. (2b-2c); there was an endothermic change and 6 % weight loss at a temperature from 30 to 225 ºC; an exothermic change and 4 % weight loss at a temperature in the range of 225-390 ºC; a big endothermic change with 6 % weight loss at a temperature in the range of 390-750 ºC; from 1000 ºC there were an endothermic change and little weight loss. The differences among Fig. (2a-2c) were that Fig. (2b-2c) had two little valleys, respectively and the weight loss gradually decreased from SSA to SSC and finally reached the least in SSC. The explanation of phenomenon above was that the evaporation of adsorbed water molecules happened below

225 ºC; there was an H_2O loss from the mixture of ceramsite in the temperature range of 225-390 ºC; from 390 to 750 ºC the carbonous materials were decomposed to release many gases, such as CO_2, CO and *etc.*; the formation of crystalline phases and some phases changes appeared after 900 ºC; owing to the content of sewage sludge gradually decreasing from SSA to SSC, the ignition loss also became less and less; the two little valleys from 800 to 1000 ºC in Fig. (2b-2c) might be due to the dehydration of silicate hydrates[11].

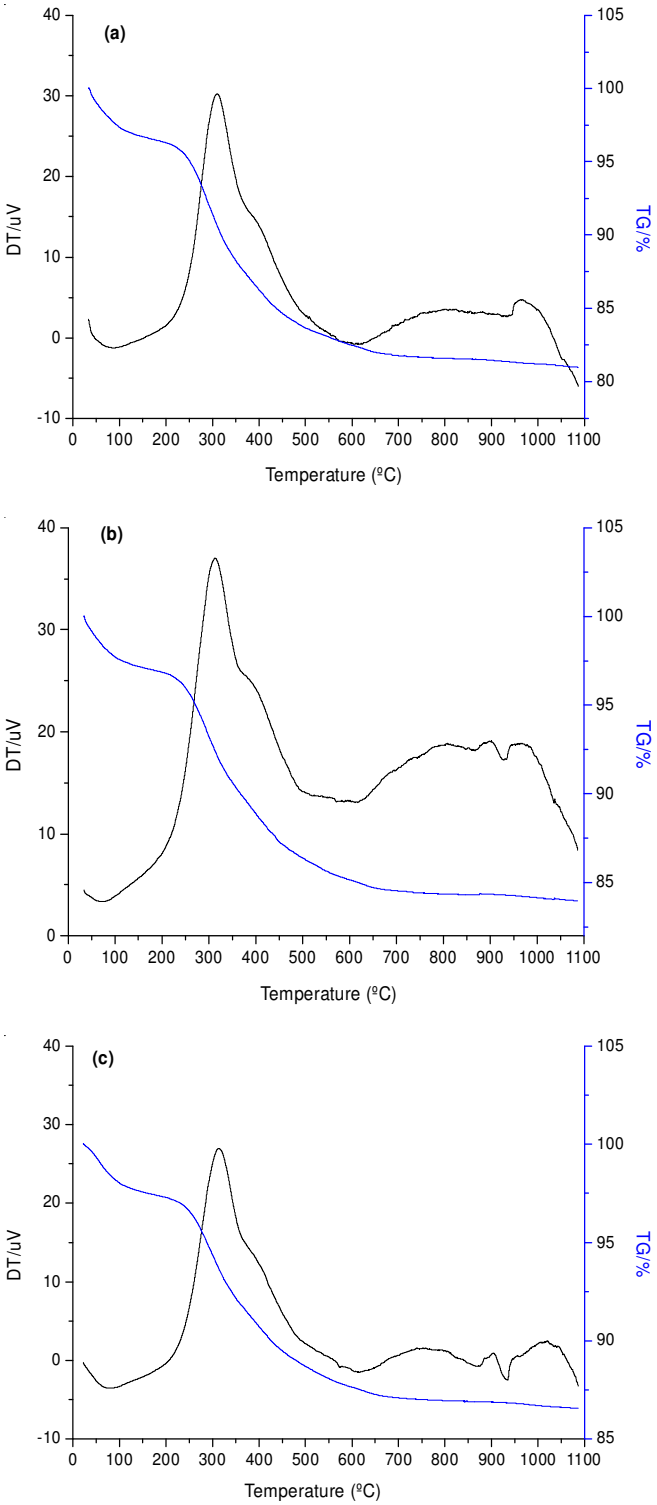

Fig. 2. a) DT-TG analyses of SSA; b) DT-TG analyses of SSB; c) DT-TG analyses of SSC

Crystalline phases and chemical composition analyses: To evaluate the effect of different sintering temperatures on the variation of crystalline phases, the example of SSE divided into 4 parts of same quality were sintered at 900, 1000, 1050, 1100 ºC, respectively under the same duration of 20 min. The results are shown in Table-4 and Fig. 3.

TABLE-4
CRYSTALLINE PHASES OF CERAMITE AT DIFFERENT SINTERING TEMPERATURES

Sintering temperature (ºC)	Major constituents
900	Silicon oxide (SiO_2) Akermanite ($Ca_2MgSi_2O_7$) Albite ($NaAlSi_3O_8$) Hematite (Fe_2O_3)
1000	Silicon oxide (SiO_2) Akermanite ($Ca_2MgSi_2O_7$) Hematite (Fe_2O_3) Albite ($NaAlSi_3O_8$)
1050	Quartz (SiO_2) Albite ($NaAlSi_3O_8$) Gehlenite [$Ca_2Al(AlSiO_7)$] Hematite (Fe_2O_3)
1100	Quartz (SiO_2) Albite ($NaAlSi_3O_8$) Gehlenite [$Ca_2Al(AlSiO_7)$] Hematite (Fe_2O_3)

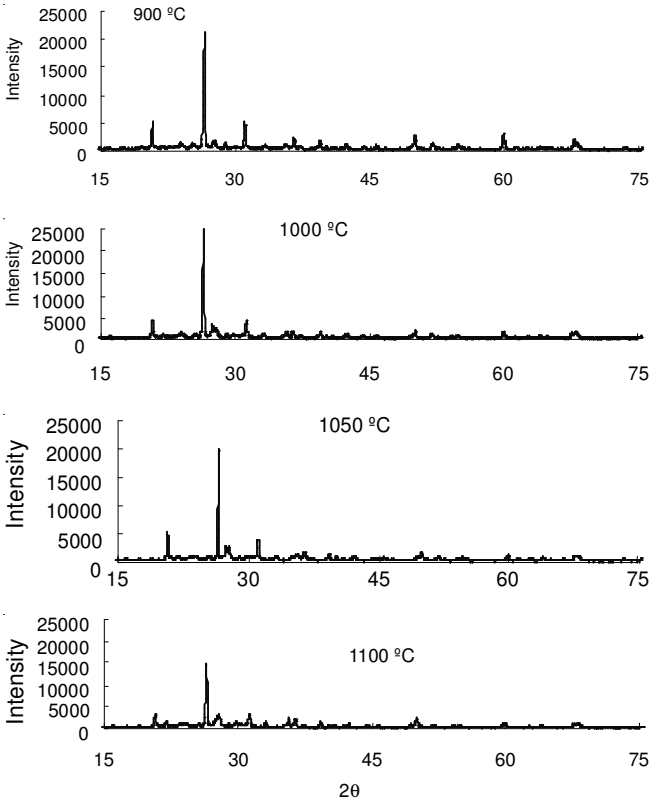

Fig. 3. X-ray diffraction of SSE at 900-1100 ºC for 20 min

It can be seen from Table-4 and Fig. 3 that the major crystalline phase was quartz (SiO_2), akermanite ($Ca_2MgSi_2O_7$), albite ($NaAlSi_3O_8$) and hematite (Fe_2O_3) at 900-1000 ºC and quartz (SiO_2), albite ($NaAlSi_3O_8$), gehlenite [$Ca_2Al(AlSiO_7)$], hematite (Fe_2O_3) were the major crystalline phases at 1050-1100 ºC; the only crystalline transformation was from

akermanite ($Ca_2MgSi_2O_7$) to gehlenite [$Ca_2Al(AlSiO_7)$]; hematite (Fe_2O_3) always existed from 900 to 1100 ºC and had no reaction with other matters to form crystalline. The crystalline phase of akermanite ($Ca_2MgSi_2O_7$) appearing at 900 ºC indicated that owing to containing many organic matters (SS), the formation of crystals happened before 900 ºC and the melting point of ceramsite manufactured from blast furnace slag, sewage sludge and clay was less than that of products produced from clay only, which was up to 1300 ºC. The more liquid phases led to the formation of more complex crystalline phases, which was thought to correspond to the endothermic changes above 900 ºC in the DT curves in 3.2[12]. Meanwhile, the variation of crystalline phases above 1050 ºC was to accord with that of pore size diameters of ceramsite in 3.1 and as the sintering temperature increased, the complicated crystals gradually formed and the pore size diameter became bigger than before. The main reactions of the transformation of crystalline phases in ceramsite might be as following:

$$2CaO + MgO + 2SiO_2 \xrightarrow{900\text{-}1000\ ^oC} Ca_2MgSi_2O_7 \quad (1)$$

$$Na_2O + Al_2O_3 + 6SiO_2 \xrightarrow{900\text{-}1100\ ^oC} 2NaAlSi_3O_8 \quad (2)$$

$$Ca_2MgSi_2O_7 \xrightarrow{1050\text{-}1100\ ^oC} 2CaO + MgO + 2SiO_2 \quad (3)$$

$$2CaO + Al_2O_3 + SiO_2 \xrightarrow{1050\text{-}1100\ ^oC} Ca_2Al(AlSiO_7) \quad (4)$$

Conclusion

Based on the results obtained in this study, the conclusions are drawn as follows: (1) With the sintering temperature and duration increasing, the pore size diameter gradually increased up to the maximum of 120 nm at 1100 ºC, 20 min and the turn point of the pore size diameter was at 1050 ºC, 20 min. Corresponding to the variation of the pore size diameter, the highest porosity of ceramsite reached 88 % while 62 % was the lowest porosity of it. (2) The effect of the different mass ratios of three raw materials on the thermal behaviours of ceramsite was very little and the curves of DT-TG mainly had the same trends of variation. (3) As the sintering temperature increased, the complex crystalline phases appeared at 900 ºC and no variation happened on the main crystalline phases except the transformation from akermanite ($Ca_2MgSi_2O_7$) to gehlenite [$Ca_2Al(AlSiO_7)$] at 1050 ºC.

ACKNOWLEDGEMENTS

The author gratefully acknowledged the financial support by the Priority Academic Program Development of Jiangsu Higher Education Institutions, China.

REFERENCES

1. A. Magrinho, F. Didelet and V. Semiao, *Waste Manage*., **26**, 1477 (2006).
2. A.B. Hizon-Fradejas, Y.C. Nakano, S.S. Nakai, W. Nishijima and M. Okada, *J. Hazard. Mater.*, **166**, 1560 (2009).
3. B. Das, S. Prakash, P.S.R. Reddy and V.N. Misra, *Resour., Conserv. Recycl.*, **50**, 40 (2007).
4. B. Kostura, H. Kulveitova and J. Lesko, *Water Res.*, **39**, 1795 (2005).
5. C. Favoni, D. Minichelli, F. Tubaro, S. Bruckner, A. Bachiorrini and S. Maschio, *Ceram. Int.*, **31**, 697 (2005).
6. G.R. Xu, J.L. Zou and G.B. Li, *J. Hazard. Mater.*, **150**, 394 (2008).
7. G.R. Xu, J.L. Zou and G.B. Li, *Water Res.*, **43**, 2885 (2009).
8. H.F. Cheng, W.P. Xu, J.L. Liu, Q.J. Zhao, Y.Q. He and G. Chen, *Ecol. Eng.*, **29**, 96 (2007).
9. H.B. Duan, Q.F. Huang, Q. Wang, B.Y. Zhou and J.H. Li, *J. Hazard. Mater.*, **158**, 221 (2008).
10. J.L. Zou, G.R. Xu and G.B. Li, *J. Hazard. Mater.*, **165**, 995 (2009).
11. L.T. Lu, T.Y. Hsiao, N.C. Shang, Y.H. Yu and H.W. Ma, *Waste Manage.*, **26**, 661 (2006).
12. R. Mohan, J. Spiby, G.S. Leonardi, A. Robins and S. Jefferis, *Public Health*, **120**, 908 (2006).
13. X.R. Wang, Y.Y. Jin, Y.F. Nie, Q.F. Huang and Q. Wang, *Waste Manage.*, **29**, 1330 (2009).
14. X.R. Wang, Y.Y. Jin, Z.Y. Wang, R.B. Mahar and Y.F. Nie, *J. Hazard. Mater.*, **160**, 489 (2008).